

## Embedding Multi-Wall Carbon Nanotubes as Conductive Nanofiller onto Bi<sub>2</sub>Te<sub>3</sub> Thermoelectric Matrix

Miguel A. S. Almeida<sup>1</sup>, João M. Magalhães<sup>2</sup>, Maria M. Maia<sup>3</sup>,  
Ana L. Pires<sup>4</sup>, André M. Pereira<sup>5</sup>





<sup>1</sup>IFIMUP-The Institute of Physics for Advanced Materials, Nanotechnology and Photonics, Department of Physics and Astronomy, Faculty of Sciences, University of Porto, Rua do Campo Alegre, 4169-007 Porto, Portugal ([miguelalmeida2199@gmail.com](mailto:miguelalmeida2199@gmail.com)); <sup>2</sup>IFIMUP-The Institute of Physics for Advanced Materials, Nanotechnology and Photonics, Department of Physics and Astronomy, Faculty of Sciences, University of Porto, Rua do Campo Alegre, 4169-007 Porto, Portugal ([j2.magalhaes@gmail.com](mailto:j2.magalhaes@gmail.com)); <sup>3</sup>IFIMUP-The Institute of Physics for Advanced Materials, Nanotechnology and Photonics, Department of Physics and Astronomy, Faculty of Sciences, University of Porto, Rua do Campo Alegre, 4169-007 Porto, Portugal ([margarida.s.maia@gmail.com](mailto:margarida.s.maia@gmail.com)); <sup>4</sup>IFIMUP-The Institute of Physics for Advanced Materials, Nanotechnology and Photonics, Department of Physics and Astronomy, Faculty of Sciences, University of Porto, Rua do Campo Alegre, 4169-007 Porto, Portugal ([ana.pires@fc.up.pt](mailto:ana.pires@fc.up.pt)) ORCID 0000-0002-6439-7946; <sup>5</sup>IFIMUP-The Institute of Physics for Advanced Materials, Nanotechnology and Photonics, Department of Physics and Astronomy, Faculty of Sciences, University of Porto, Rua do Campo Alegre, 4169-007 Porto, Portugal ([ampereira@fc.up.pt](mailto:ampereira@fc.up.pt)) ORCID 0000-0002-8587-262X

### Abstract

Thermoelectric Generators (TEGs) are devices that have the ability to directly convert heat into electrical power, or vice-versa, and are being envisaged as one off-the-grid power source. Furthermore, carbon-based materials have been used as a conducting filler to improve several properties in thermoelectric materials. The present work studied the influence on the thermoelectric performance of Bi<sub>2</sub>Te<sub>3</sub> bulk materials by incorporating different concentrations of Multi-Walled Carbon Nanotubes (MWCNT). In order to control and understand the influence of MWCNT dispersion in the nanocomposite, two different production methods (manual grinding and ultrasonication) were carried out and compared. It was verified that a larger dispersion leads to a better outcome for thermoelectric performance. The achieved Seebeck coefficient was up to -162 μV K<sup>-1</sup> with a Power Factor of 0.50 μW K<sup>-2</sup>m<sup>-1</sup>, for the nanocomposite produced with 11.8 %V of MWCNT. This result demonstrates the ability to increase the thermoelectric performance of Bi<sub>2</sub>Te<sub>3</sub> throughout the addition of MWCNT.

**Author Keywords.** Thermoelectric Generators, Bi<sub>2</sub>Te<sub>3</sub>, MWCNT, Nanocomposites.

**Type:** Research Article

 Open Access  Peer Reviewed   CC BY

### 1. Introduction

Humankind is continuously growing and evolving at a steady pace. Consequently, it is crucial to find new approaches to energy production using renewable methods to convert all the wasted energy into usable one. Over than 50% of all energy used is converted into waste heat to the environment, so harvesting this waste energy and converting it into useful energy is a must (Johnson, Choate, and Davidson 2008). In this framework, the thermoelectric (TE) materials could play an essential role in the energy production and recovery.

The TE effect can be described as the direct conversion of a temperature difference to an electrical voltage, or vice versa. When a TE material is subjected to a temperature gradient, the energy of the conduction band will also experience a gradient, and the charge carriers of

the hot side, with higher energy, will tend to diffuse to the cold side, towards a steady low energy state. This leads to a build-up of charges that gives origin to electrostatic potential (Shi, Zou, and Chen 2020). In the case of a TE device that is composed of n-type and p-type semiconductors, that contain electrons and holes, respectively, the two types of charge carriers will tend to diffuse to the cold side (Freer and Powell 2020). In order to infer and evaluate the efficiency of a material, there is a parametrization with respect to the TE performance, the so-called figure of merit ZT:

$$ZT = \frac{S^2\sigma}{\kappa} T = \frac{PF}{\kappa} T \quad (1)$$

where S is the Seebeck coefficient,  $\sigma$  is the electrical conductivity, and  $\kappa$  is the thermal conductivity. The Power Factor (PF) given by  $S^2\sigma$ , allows to infer about the energy bands changes of the material (Hamid Elsheikh et al. 2014).

However, these transport properties depend on interrelated material features such as the charge carrier concentration (Ma et al. 2021). Consequently, the search for new materials with high PF and low  $\kappa$ , to increase the ZT, has become the main objective of this field. Several efforts have already been made to enhance the interdependence of the TE properties, such as processing conditions, nanostructuring, texture alignment, point defect engineering, and bandgap enlargement (Ma et al. 2021; Hong, Chen, and Zou 2018). From all implemented techniques in the Bi<sub>2</sub>Te<sub>3</sub> alloys (the material with higher ZT at room temperature), the nano-compositing, nano-confinement, and nano-structuring revealed several advantages. The nanostructured TE material creates several new boundaries that cause phonon scattering due to the lattice mismatch and the vibrational difference, thus leading to a decrease in the  $\kappa$ . However, the nanostructures can have a negative impact on the  $\sigma$  since the electrons are also scattered in the grain boundaries. Therefore, the introduction of nanomaterials in the micrometric matrix of the TE materials, for the production of nanocomposites, has been increasingly implemented (Zhang et al. 2015). Nanocomposites, appear as a good methodology relative to others currently being used because are simple to deploy, low-cost, and capable of being implemented on a commercial scale (El-Makaty, Ahmed, and Youssef 2021).

The introduction of nanomaterials, such as MWCNT, still allows the reduction of the thermal conductivity due to the lattice phonon and carrier scattering originated on the MWCNT/Bi<sub>2</sub>Te<sub>3</sub> interface, which decreases the lattice thermal conductivity (Kumar, Chaudhary, and Khare 2019), but with a simultaneous increase of the S due to a higher percolation and to the electron energy filtering effect (Zhang et al. 2015). This effect prevents the passage of charges with low energy due to the formation of an energy barrier in the conduction band, acting as an energy filter. Thus, only high-energy charges are able to pass through, inducing an increase in the average energy of the charge carriers and, consequently, an increase in the S value (Nandihalli, Liu, and Mori 2020). In this way, the increase of the S value can compensate for any decrease in the  $\sigma$ , allowing to preserve or increase the PF (Zhang et al. 2015). For that reason, the nanocomposites enable an increase in  $\sigma$  and S, along with a decrease in  $\kappa$ , thus leading to an increase in ZT with the advantage of better thermal stability (El-Makaty, Ahmed, and Youssef 2021; Jagadish et al. 2019).

There are several challenges in the application of MWCNT, such as scattering and cluster formation, which can lead to the formation of undesirable effects that decrease the Seebeck coefficient and the energy filtering effect. One of the main reasons for cluster formation is the use of high concentrations of MWCNTs where, for example, at 0.10 %Wt the MWCNT are well

dispersed, in a Bi<sub>2</sub>Te<sub>3</sub> polymeric matrix, but at 0.20 %Wt the MWCNT start to form clusters at various locations, leading to a detrimental effect (Jagadish et al. 2019).

Accordingly, the ultimate aim of this work is to carry out a systematic survey of a TE material formed by a nanocomposite of Bi<sub>2</sub>Te<sub>3</sub> with MWCNT functioning as nanofillers to understand where the threshold concentration of MWCNT is located to achieve the best performance in the thermal to electrical conversion.

## 2. Materials and Methods

### 2.1. Materials preparation

Commercial MWCNT were acquired from the Nanocyl SA, NC7000TM, with 9.5 nm and 1.5 μm of average diameter and length, respectively (Nanocyl, n.d). The thermoelectric powder from this work uses Bi<sub>2</sub>Te<sub>3</sub>, from commercial Peltier modules, that was ball-milled and sieved to obtain a mean size of 10-50 μm.

Regarding the methodologies for the mixing of both powders, two different methods were used in order to compare the influence of the nanotube's dispersion. The first technique only comprises the use of manual grinding resorting to a mortar, whereas the second technique adds up a second step after grinding which is an ultrasound bath using an ethanol solution. Concerning the ultrasound bath, it was carried out for 10 minutes in a Retsch-UR1 ultrasound at a frequency of 35 kHz, and 2x240 W. The solution is then placed in an incubator for 4 hours at 50°C, in order to evaporate all the liquid solution. Afterward, were produced pellets of 1.3 cm in diameter resorting to a press machine by applying a pressure of 2000 psi for 60 seconds at room temperature. This procedure allows obtaining several pellets in different concentrations of MWCNT and Bi<sub>2</sub>Te<sub>3</sub> for further characterization.

### 2.2. Characterization techniques

The transport properties were performed towards obtaining the  $S$  and  $\sigma$ . Regarding the measurement of  $S$ , was used a homemade setup (Pires et al. 2019). The electrical conductivity was obtained by measuring the resistivity of samples using the four-point method. The correct resistivity value,  $\rho$ , is obtained by taking into account the shape factor correction, due to the cylindrical geometry of the pellet. Therefore, by determining the distance between the probes,  $s$ , and the thickness of the samples,  $t$ , it is possible to obtain the resistivity value through Equation (2) (Pires et al. 2019).

$$\rho = \frac{V}{I} \frac{\pi t}{\ln\left(\frac{\sinh(t/s)}{\sinh(t/2s)}\right)} \quad (1)$$

The conductivity value can be obtained from the resistivity value ( $\sigma = 1/\rho$ ). With these measured values it is now possible to obtain the PF for all different samples.

In addition to the transport properties, was performed a crystallographic analysis of the samples using X-ray analysis in the Smartlab Rigaku diffractometer. The configuration used was a Bragg-Brentano  $\theta/2\theta$  using Cu K $\alpha$  radiation ( $\lambda = 1.540593\text{\AA}$ ) at room temperature.

## 3. Discussion

In this work were used different ratios of MWCNT and n-type Bi<sub>2</sub>Te<sub>3</sub>. The materials were mixed at concentrations of 0, 0.1, 0.25, 0.5 and 0.75 %Wt of MWCNT which corresponds to 0, 4.9, 11.8, 20.5, and 28.1 %V of MWCNT. Two different sets of samples were made: the first set (Set1) of samples was produced using only manual grinding, while the second (Set2) was produced using manual grinding and the ultrasound technique.

In **Figure 1a)** is shown the amplified image of the pellet composed of grains of this powder with a micrometer diameter (Bi<sub>2</sub>Te<sub>3</sub>), using a digital optical microscope. The analysis of different concentrations, within the same set, and different techniques, between sets, aims to determine the optimized concentration of nanotubes and to analyze the influence of good dispersion on the obtained results, respectively.

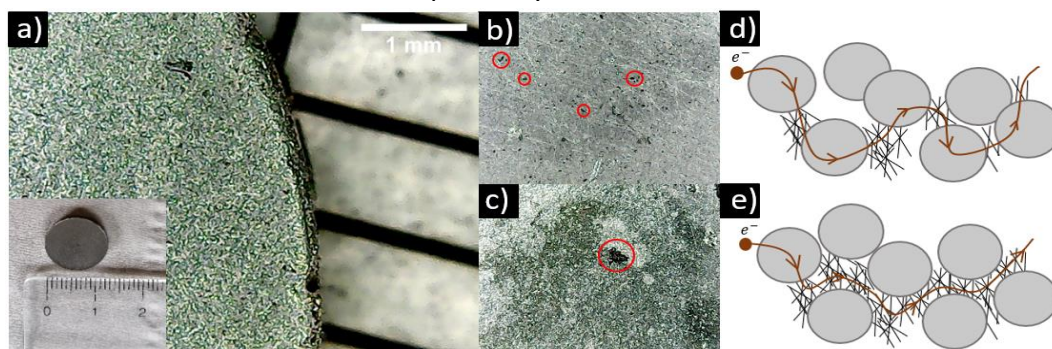


**Figure 1:** a) Pellet image (0.10 %Wt MWCNT) with, and without, optical microscope amplification; b) Amplified image of the pellet with 0.10 %Wt of MWCNT, showing small black dots resulting from agglomerations of MWCNT; c) Amplified pellet image with 0.75 %Wt of MWCNT, with a large agglomeration of MWCNT; d) Path taken by electrons with poor dispersion and e) good dispersion of nanotubes

In order to establish the crystallographic structure of the samples, X-ray analysis was performed as shown in **Figure 2**. In **Figure 2a)** is possible to compare the diffractograms of different composites samples and the corresponding precursors (Bi<sub>2</sub>Te<sub>3</sub> and MWCNT), and in **Figure 2b)** the diffractograms of samples from different sets. On the MWCNT diffraction pattern (inset graph of **Figure 2b)** is possible to observe that the most intense diffracted peak occurs at  $2\theta = 25.7^\circ$ , corresponding to the (002) miller index, and the second most intense one occurs at  $2\theta = 42.8^\circ$ , corresponding to the (100) plane. When compared the position of the peaks on **Figure 2a)**, it is not possible to verify the MWCNT peaks due to the low intensity and low concentration, in relation to the concentration of Bi<sub>2</sub>Te<sub>3</sub>, as was already indicated.

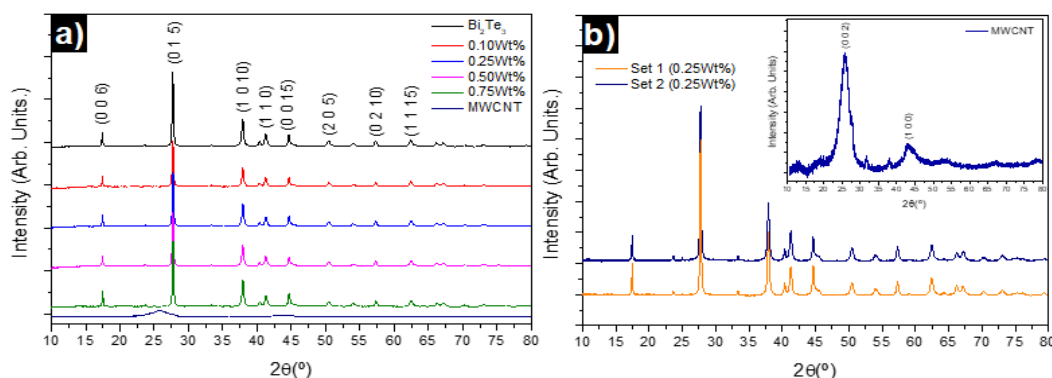


**Figure 2:** X-ray diffraction patterns. Comparison between the patterns: a) MWCNT, Bi<sub>2</sub>Te<sub>3</sub>, and the different concentration samples developed for Set1 (0.1, 0.25, 0.5, 0.75 %Wt of MWCNT); b) Samples with 0.25%Wt from Set1 and Set2. Inset graph: X-ray diffraction pattern of MWCNT

Regarding the Bi<sub>2</sub>Te<sub>3</sub> diffractogram, the existence of several well-defined Bragg reflections indicates the polycrystalline characteristic of the sample, where the Bi<sub>2</sub>Te<sub>3</sub> phase was identified with the rhombohedral R $\bar{3}$ m space-group structure (Pires et al. 2019) as can be confirmed by the main peaks at  $2\theta = 27.7^\circ$  (0 1 5),  $2\theta = 37.8^\circ$  (1 0 10), and  $2\theta = 44.1^\circ$  (0 0 15). Comparing the samples from the same Set and different Sets, there is no variation in the position of the peaks or in relative intensities, which indicates that the addition of MWCNT

and the methods of production of the samples are not interfering with the crystal structure of the TE powder.

The transport properties of the different samples were also measured. To grasp the MWCNTs impact on  $S$  and  $\sigma$ , two pellets composed only of one constituent (Bi<sub>2</sub>Te<sub>3</sub> and MWCNTs) were produced for standardization, under the same conditions (pressure and temperature). Regarding the Bi<sub>2</sub>Te<sub>3</sub>, was possible to achieve a value of  $S = -150 \mu\text{V K}^{-1}$  and  $\sigma = 21.86 \text{ S m}^{-1}$ , while the MWCNT had  $S = 4 \mu\text{V K}^{-1}$  and  $\sigma = 39.67 \text{ S m}^{-1}$ . These results highlight the n-type nature of the Bi<sub>2</sub>Te<sub>3</sub>, and p-type nature of the MWCNT, along with the higher  $\sigma$  of the former material. The obtained results for the remaining samples are shown in Figure 3, as function of the volumetric concentration of MWCNT relative to the Bi<sub>2</sub>Te<sub>3</sub>.

Starting with the analysis of  $S$  (Figure 3a) it is possible to verify in both sets an increase in the absolute value of  $S$ ,  $|S|$ , followed by a decrease in the value. In the case of Set1, the variation in the value of  $S$  shows a more erratic behavior that stems from the clustering of MWCNTs due to their strong electrostatic surface interaction. This behavior is confirmed by the measurements of the samples in Set2, where the mixture promotes the spread of MWCNT and Bi<sub>2</sub>Te<sub>3</sub>, leading to a better dispersion and trend. This finding is backed up by previous work, undertaken by Jagadish et al. (2019), where was found that the agglomeration of MWCNT can lead to the disappearance of the filtering effect. From the microscope picture, namely Figure 1b) and Figure 1c), it is possible to notice that with an increase of MWCNT concentration there is a further agglomeration and the formation of clusters. The impact on the  $S$  value relies on its maximum absolute value for 11.8 %V of MWCNT, being  $-158 \mu\text{V K}^{-1}$  and  $-162 \mu\text{V K}^{-1}$  for Set1 and Set2, respectively.

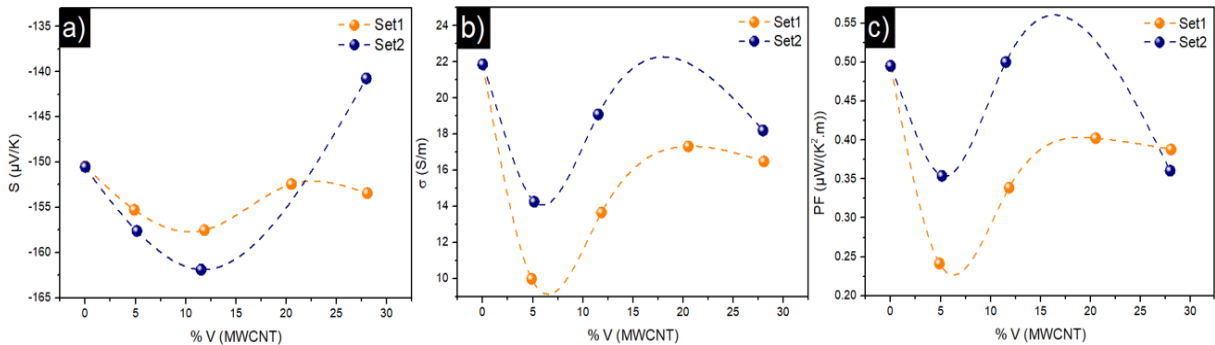


**Figure 3:** Transport properties of the different groups of samples: a) Seebeck coefficient; b) Electrical conductivity; c) Power Factor

Regarding  $\sigma$ , since is a short-range method and sensitive to defects, such as the grain boundary scattering (contrary to  $S$  which depends on the density of states), the behavior is more complex. Although, a good conductive material is being incorporated the TE matrix, it can be observed, in Figure 3b), that the value of  $\sigma$  does not increase as intended, but declines for any concentration of carbon nanotubes. However, the Seebeck coefficient behavior confirms that filtering effect is occurring. As was said before, the filtering effect allows to increase the average energy of the charges by filtering the charges with lower energy and helps to increase the  $|S|$  value, although it leads to a decrease in the concentration of charges in the material ( $n$ ) (El-Makaty, Ahmed, and Youssef 2021). Considering that the conductivity is directly proportional to  $n$  ( $\sigma = nq\mu$ ), this filtering process leads to a decrease of  $\sigma$ . With the increase in the concentration and agglomeration of the MWCNT, the filtering effect ceases to exist, increasing again the value of  $n$  and  $\sigma$  (Jagadish et al. 2019). There are other phenomena that are correlated, such as the contact resistance and percolation through the material, that is related to the use of a simple dispersion technique with no control over the organization of

the microstructure. The contact resistance is due to the use of a micrometric TE powder mixed with nanometric structures, leading to a contact resistance in the passage between the two materials. Agglomeration or low concentration of MWCNT can prevent percolation through the material, inducing a high interface resistance between materials and a consequent increase in electrical resistance. However, as can be observed in the [Figure 1d](#)) and [Figure 1e](#)), a better dispersion of the MWCNT, and the appearance of percolation leads to an increase in  $\sigma$  when compared to the previous case. This outcome can be assumed because between each individual microparticle it is embedded a collection of nanotubes that will allow the percolation of electrons throughout the sample. Comparing the information in [Figure 3b](#)) with the explanations above, it is possible to confirm that with a larger concentration of nanotubes (within the same set) or larger dispersion (between sets), the  $\sigma$  of the sample is higher.

Finally, it is possible to obtain the value of the PF from the values discussed above. Regarding the Set1 of samples, it was verified that the PF value is strongly influenced by the drop in  $\sigma$  since the variation in  $S$  is not significant. However, in Set2 of samples, the drop in  $\sigma$  is smaller and the increase in  $|S|$  is higher, which results in an increase of PF value and in a higher TE performance of this group of samples. This is in agreement with previous results present in the literature. [Jagadish et al. \(2019\)](#) also found a similar increase of  $|S|$  followed by a decrease of this value, obtaining an optimized value of  $-70\mu\text{VK}^{-1}$  to 0.1wt% of MWCNT. Regarding to the value of  $\sigma$ , the behavior observed is strongly influenced by the poor dispersion of CNTs, and in the literature the best results was obtained using more complex techniques, such as long times on ultrasounds ([Jagadish et al. 2019](#)) or hydrothermal synthesis ([Kumar, Chaudhary, and Khare 2019](#)). However, these methods can become expensive, and it is necessary to find more accessible techniques. In the samples where was used the ultrasounds, it was possible to find an optimal concentration of 11.8 %V of MWCNT to achieve an increase in the PF to  $0.50\mu\text{W K}^{-2}\text{m}^{-1}$ , which is higher than the samples without the implementation of MWCNT.

#### 4. Conclusions

The use of the ultrasound method, for the two sets of samples, was successfully applied and lead to a higher dispersion of the MWCNT. In the obtained results was possible to observe the filtering effect, that increases the absolute value of the  $S$  value but can decrease the concentration of charge carriers in the sample. However, the high charge mobility in the MWCNT can compensate for this loss, which can lead to an increase in the  $\sigma$ .

Resorting to the transport proprieties characterization, was reached an optimal concentration of 11.8 %V of MWCNT in Set2, where was obtained a  $S$  of  $-162\mu\text{VK}^{-1}$  and a PF of  $0.50\mu\text{WK}^{-2}\text{m}^{-1}$ . This result demonstrates that is possible to achieve an increase in the final thermoelectric performance throughout the implementation of MWCNT in a Bi<sub>2</sub>Te<sub>3</sub> matrix. For future work, the mixing techniques of these two powders should be optimized, in order to reduce the resistance between the different materials. In addition, the influence of the size of the Bi<sub>2</sub>Te<sub>3</sub> grains on the results obtained can also be analyzed.

#### References

El-Makaty, F. M., H. K. Ahmed, and K. M. Youssef. 2021. "The effect of different nanofiller materials on the thermoelectric behavior of bismuth telluride". *Materials and Design* 209: Article number 109974. <https://doi.org/10.1016/j.matdes.2021.109974>.

- Freer, R., and A. V. Powell. 2020. "Realising the potential of thermoelectric technology: A Roadmap". *Journal of Materials Chemistry C* 8, no. 2: 441-63. <https://doi.org/10.1039/c9tc05710b>.
- Hamid Elsheikh, M., D. A. Shnawah, M. F. M. Sabri, S. B. M. Said, M. Haji Hassan, M. B. Ali Bashir, and M. Mohamad. 2014. "A review on thermoelectric renewable energy: Principle parameters that affect their performance". *Renewable and Sustainable Energy Reviews* 30: 337-55. <https://doi.org/10.1016/j.rser.2013.10.027>.
- Hong, M., Z. G. Chen, and J. Zou. 2018. "Fundamental and progress of Bi<sub>2</sub>Te<sub>3</sub>-based thermoelectric materials". *Chinese Physics B* 27, no. 4: Article number 048403. <https://doi.org/10.1088/1674-1056/27/4/048403>.
- Jagadish, P., M. Khalid, N. Amin, M. T. Hajibeigy, L. P. Li, A. Numan, N. M. Mubarak, R. Walvekar, and A. Chan. 2019. "Recycled carbon fibre/Bi<sub>2</sub>Te<sub>3</sub> and Bi<sub>2</sub>S<sub>3</sub> hybrid composite doped with MWCNTs for thermoelectric applications". *Composites Part B: Engineering* 175: Article number 107085. <https://doi.org/10.1016/j.compositesb.2019.107085>.
- Johnson, I., W. Choate, and A. Davidson. 2008. *Waste Heat Recovery. Technology and opportunities in U.S. Industry*. United States: U.S Department of Energy - Office of Scientific and Technical Information. <https://doi.org/10.2172/1218716>.
- Kumar, S., D. Chaudhary, and N. Khare. 2019. "Enhanced thermoelectric figure of merit in Bi<sub>2</sub>Te<sub>3</sub>-CNT-PEDOT nanocomposite by introducing conducting interfaces in Bi<sub>2</sub>Te<sub>3</sub> nanostructures". *APL Materials* 7, no. 8: Article number 081123. <https://doi.org/10.1063/1.5087550>.
- Ma, Z., J. Wei, P. Song, M. Zhang, L. Yang, J. Ma, W. Liu, F. Yang, and X. Wang. 2021. "Review of experimental approaches for improving zT of thermoelectric materials". *Materials Science in Semiconductor Processing* 121: Article number 105303. <https://doi.org/10.1016/j.mssp.2020.105303>.
- Nandihalli, N., C. J. Liu, and T. Mori. 2020. "Polymer based thermoelectric nanocomposite materials and devices: Fabrication and characteristics". *Nano Energy* 78: Article number 105186. <https://doi.org/10.1016/j.nanoen.2020.105186>.
- Nanocyl. n.d. "NC7000™ Industrial multiwall carbon nanotubes". Accessed May 10, 2021. <https://www.nanocyl.com/product/nc7000/>.
- Pires, A. L., I. F. Cruz, J. Silva, G. N. P. Oliveira, S. Ferreira-Teixeira, A. M. L. Lopes, J. P. Araújo, J. Fonseca, C. Pereira, and A. M. Pereira. 2019. "Printed flexible μ-thermoelectric device based on hybrid Bi<sub>2</sub>Te<sub>3</sub> /PVA composites". *ACS Applied Materials and Interfaces* 11, no. 9: 8969-81. <https://doi.org/10.1021/acsami.8b18081>.
- Shi, X. L., J. Zou, and Z. G. Chen. 2020. "Advanced thermoelectric design: From materials and structures to devices". *Chemical Reviews* 120, no. 15: 7399-515. <https://doi.org/10.1021/acs.chemrev.0c00026>.
- Zhang, Q., X. Ai, L. Wang, Y. Chang, W. Luo, W. Jiang, and L. Chen. 2015. "Improved thermoelectric performance of silver nanoparticles-dispersed Bi<sub>2</sub>Te<sub>3</sub> composites deriving from hierarchical two-phased heterostructure". *Advanced Functional Materials* 25, no. 6: 966-76. <https://doi.org/10.1002/adfm.201402663>.

## Acknowledgments

MSA, JQM, ALP and AMP thank the funding from the European Union's Horizon 2020 Research and Innovation Programme under Grant Agreement No. 863307 (Ref. H2020-FETOPEN-2018-2019- 2020-01). MMM thanks FCT for grant SFRH/BD/144229/2019.